EPS-HEP99
Abstract # 1-410
Parallel sessions: 1,5
Plenary sessions: 1,5
ALEPH 99-023
CONF 99-018
June 29, 1999

P R E L I M I N A R Y

QCD studies with e^+e^- annihilation data at 189 GeV

The ALEPH Collaboration

Contact person : G. Dissertori, Guenther.Dissertori@cern.ch

Abstract

Properties of hadronic events produced at LEP at centre-of-mass energy of 189 GeV are studied and compared with QCD predictions. Distributions of event-shape observables, jet rates and multiplicities are presented and compared to the predictions of several Monte Carlo models and analytic QCD calculations. From a fit of $\mathcal{O}(\alpha_s^2)$+NLLA QCD calculations to distributions of event-shape variables, α_s has been determined.

Contribution by ALEPH to the 1999 summer conferences

1 Introduction

Studies of the production of hadronic events collected by the ALEPH detector at LEP at 189 GeV centre-of-mass energy are presented.

The general ideas remain essentially those of [1]. The primary goal is to investigate quantities for which the centre-of-mass energy dependence is well predicted by QCD. By comparing with corresponding measurements based on the data collected at $E_{\rm cm} = M_{\rm Z}$ and also at lower energies, the predictions can be tested. An additional goal of the measurements is to provide a check of QCD-based Monte Carlo models; these are used for estimating backgrounds and efficiencies in many other analyses such as in searches for new particles and in studies of the W boson.

The observables include inclusive charged particle distributions, jet rates, and distributions of event-shape variables. These are compared to QCD predictions, either from QCD-based models or analytic QCD formulae. In addition, a number of quantities are measured such as the mean multiplicity of charged particles, moments of event-shape variables, and the strong coupling constant α_s. The energy dependence of these quantities is investigated by comparing with corresponding measurements at lower $E_{\rm cm}$.

2 Experimental procedure

A detailed description of the ALEPH detector is given in [2]. The measurements presented here are based on both charged particle measurements from the time projection chamber, inner tracking chamber, and vertex detector, as well as information on neutral particles from the electromagnetic and hadronic calorimeters. An energy-flow reconstruction algorithm is applied, which takes advantage of the redundancy of energy and momentum measurements and exploits photon, electron and muon identification [3]. The output of this algorithm is a list of 'energy-flow objects', with measured momentum vectors and information on particle type.

Hadronic events with large initial state photon radiation (ISR) are removed from the data sample. To separate ISR photons observed in the detector from the hadronic system, the particles in the event are clustered using the Durham algorithm [4] with a resolution parameter of $y_{\rm cut} = 0.002$. Jets are selected in which the fraction of the jet's energy carried by charged hadrons is less than 10%. From these 'electromagnetic jets', the photons and any identified electrons (or positrons) are removed; the latter are often the result of photon conversion in the material before the tracking chambers. From the remaining particles, the invariant mass $M_{\rm vis}$ and the absolute value of the sum of the p_z components are computed and the following condition is required:

$$M_{\rm vis} - |\sum p_z| \geq 0.75\sqrt{s}.$$

According to Monte Carlo studies based on the PYTHIA generator version 5.7 [5], the fraction of radiative events (defined by $\sqrt{s'/s} \leq 0.9$) in the selected sample is $\sim 4\%$.

The measurements of the various quantities use all reconstructed particles of the accepted events, including those which had previously been removed for purposes of computing $\rm M_{vis}$.

The events passing the anti-ISR cuts still contain some background from four-fermion processes (WW, ZZ, Zγ^*). These are rejected by first clustering the particles to exactly four jets with the Durham algorithm. The energies of the jets are then rescaled, keeping their directions constant, such that the total energy of the event is equal to $E_{\rm cm}$ and the total momentum is zero. The quantities

$$d^2 = \min \left[\frac{(m_{ij} - M_W)^2 + (m_{kl} - M_{\rm W})^2}{M_W^2} \right] ,$$

with $M_{\rm W}$= 80.25 GeV, and

$$c_{WW} = \cos(\text{smallest interjet angle})$$

are then computed, where for d^2 the minimum value is taken among all possible choices of jet pairings ij and kl. Events are then accepted if $d^2 \geq 0.1$ or $c_{WW} \geq 0.9$.

The integrated luminosities and numbers of events accepted and expected are shown in Table 1. The expected number of events has been obtained from the program KORALZ [6] and those for WW background from KORALW [7] and for ZZ and Zγ^* background from PYTHIA.

Table 1: Integrated luminosities and numbers of accepted and expected events. There is an uncertainty of 2% in the predicted numbers of events.

$E_{\rm cm}$ (GeV)	$\int L\,dt$ ($\rm pb^{-1}$)	events found	events expected	expected signal	expected background
189	174.2	3048	3034	2703	331

Corrections for imperfections of the detector and for the residual effects of ISR are made by means of multiplicative factors, as done in [1]. These factors, which are derived from the Monte Carlo model PYTHIA, are by construction approximately independent of the model used. For the simulation of hadronic final states in $\rm e^+e^-$ annihilation, JETSET version 7.4 [5] and PYTHIA are essentially equivalent. PYTHIA is used for the detector corrections because of its more accurate description of initial state photon radiation.

The detector systematics were, when appropriate, estimated using the Z data collected in the same year as the high-energy data. The selection cuts on track parameters were changed in the Monte Carlo until the number of events selected per unit luminosity were the same in Monte Carlo and data. These changes were then applied for Monte Carlo only to the analysis of the high-energy events, and the change in the extracted values for each event-shape variable is taken as a systematic uncertainty.

For the systematic tests of the ISR and WW rejection and the event selection cuts, performed via cut variations, various Monte Carlo samples had been generated to estimate the statistical precision of the test. The dispersion of the results for a given test applied to the Monte Carlo samples was then compared with the result of the same test applied to data. If the change in data was greater than the expected precision then it was taken as a systematic error after the statistical precision had been subtracted in quadrature. For the cases where the data test was not significant, the largest upwards and downwards fluctuations were noted. Assuming a uniform

probability distribution for this difference, an additional uncorrelated systematic uncertainty was derived.

The systematic uncertainty due to a residual model dependence has been estimated by comparing with the results based on correction factors derived from HERWIG version 5.9 [8].

Variations in the WW cross sections used for background subtraction by $\pm 2\%$ led to negligible uncertainties in the corrected distributions.

In the event-shape distributions, the systematic uncertainty estimates in each bin are dominated by the small changes in the selected events and tracks as cuts are varied, and hence are very much limited in statistical precision. For this reason, the estimates for neighbouring bins have been averaged in groups of three.

3 Inclusive charged particle distributions

Charged particle inclusive distributions were measured for the transverse momentum components in and out of the event plane defined by the thrust and major axes, $p_\perp^{\rm in}$ and $p_\perp^{\rm out}$, and the variables $\xi = -\ln x_p$, where $x_p = p/p_{\rm beam}$, and the rapidity $y = \frac{1}{2}\ln(E+p_\parallel)/(E-p_\parallel)$ with $p_\parallel$ measured with respect to the thrust axis. The thrust axis used for rapidity and the event plane used for $p_\perp^{\rm in}$ and $p_\perp^{\rm out}$ are determined using both charged and neutral particles.

Corrected inclusive distributions of $p_\perp^{in}$, $p_\perp^{out}$, y, and ξ are shown in Fig. 1, along with the predictions of the models PYTHIA version 5.7 and HERWIG version 5.9, with initial state radiation turned off. The fragmentation and QCD parameters of the models have been tuned using data from $E_{cm} = 91.2$ GeV [9].

By integrating the rapidity distribution, the mean multiplicity of charged particles, $N_{\rm ch}$, has been determined as:

$$N_{\rm ch} = 27.37 \pm 0.20_{stat} \pm 0.25_{sys}.$$

The multiplicities measured at various centre-of-mass energies are shown in Fig. 2 along with measurements from other experiments [10] and also with the predictions of the Monte Carlo models PYTHIA and HERWIG.

4 Event shapes

The various distributions describing the event shapes are of interest for several reasons. Most of the variables are predicted to second order in QCD; some can also be resummed to all orders in α_s. By fitting the theoretical predictions to these distributions the value of the strong coupling constant may be determined. By comparing with the direct predictions for the various Monte Carlo models, the validity of each model is tested.

In performing these determinations, the primary objective is to observe the running of the coupling with centre-of-mass energy; for this reason, the analyses at each energy point are designed, as far as possible, to be coherent with each other and to have correlated systematic errors.

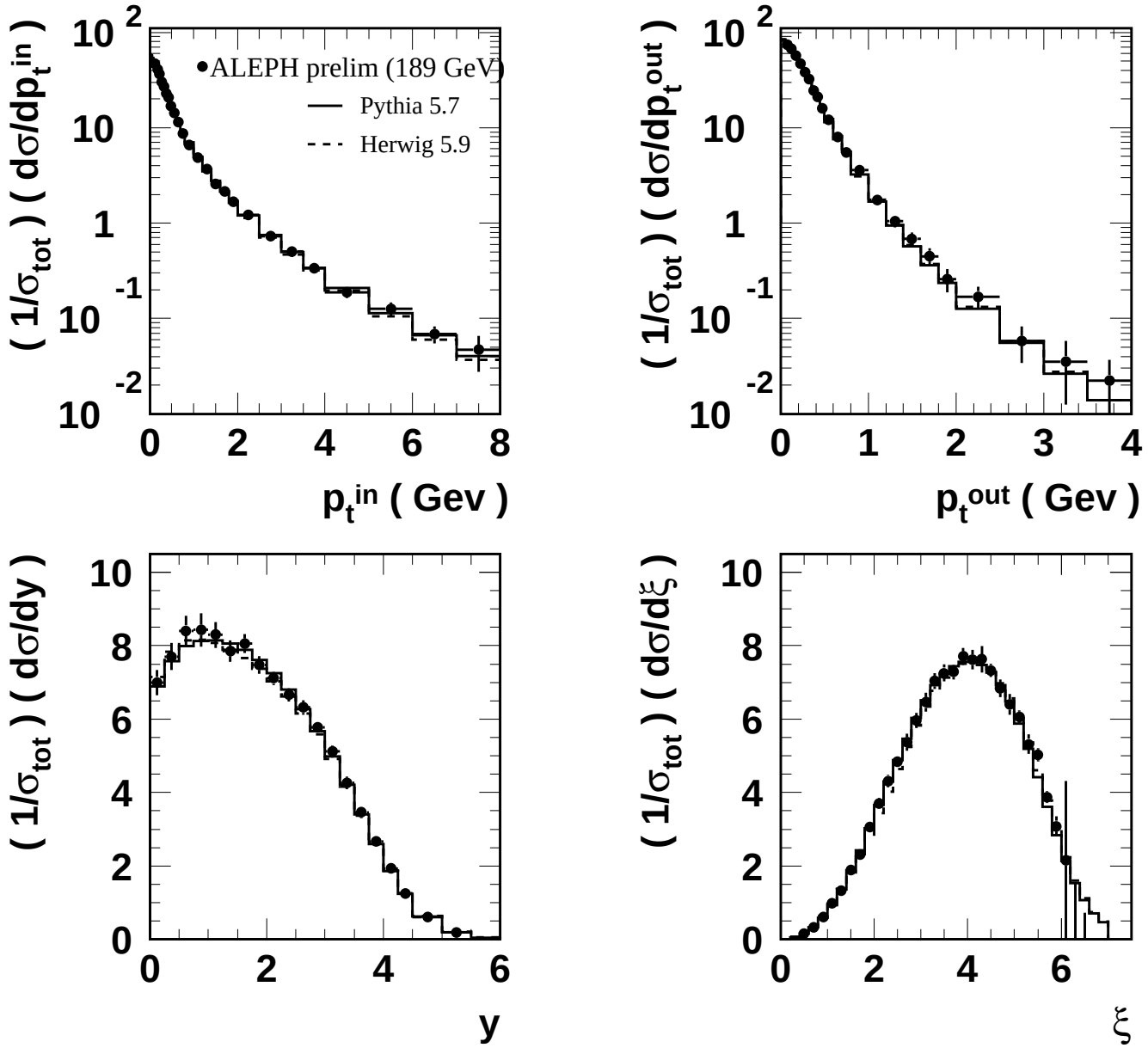

Figure 1: Distributions of $p_\perp^{in}$, $p_\perp^{out}$, rapidity y, and $\xi = -\ln x_p$ at 189 GeV. The error bars correspond to the quadratic sum of statistical and systematic uncertainties.

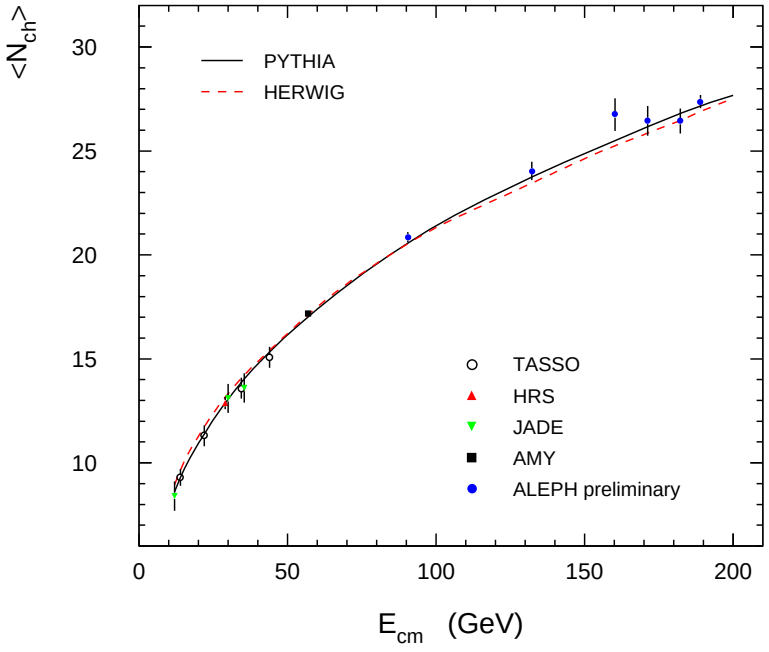

Figure 2: The mean charged particle multiplicity $N_{\rm ch}$ as a function of centre-of-mass energy $E_{\rm cm}$.

The event-shape variables studied are as follows:

Thrust T: The thrust axis $\vec{n}_T$ is along the direction $\vec{n}$ which maximises the following quantity:

$$T = \left(\frac{\sum_i |\vec{p}_i \cdot \vec{n}|}{\sum_i |\vec{p}_i|} \right) \quad , \tag{1}$$

where the sum extends over all particles in the event. The magnitude of the thrust vector is defined as the value of the expression after maximisation.

Thrust major $T_{\rm major}$: The thrust major vector, $\vec{T}_{T_{\rm major}}$, is defined in the same way as the thrust vector, but with the additional condition that $\vec{n}$ must lie in the plane perpendicular to $\vec{n}_T$.

Thrust minor $T_{\rm minor}$: The thrust minor vector is again defined in the same way as the thrust vector but with the extra constraint that $\vec{n}_{T_{\rm minor}}$ be perpendicular both to $\vec{n}_T$ and to $\vec{n}_{T_{\rm major}}$.

Oblateness O: The oblateness is defined by $O = T_{\rm major} - T_{\rm minor}$.

Heavy Jet Mass M_h^2/s: A plane through the origin and perpendicular to $\vec{n}_T$ divides the event into two hemispheres, H_1 and H_2, from which one obtains corresponding hemisphere invariant masses. The larger of the two is called the heavy jet mass, M_h. In fact, the distribution of M_h^2/s is reported; this is to first order equal to $1 - T$.

Jet Broadening variables B_t and B_w: A measure of the broadening of particles in transverse momentum with respect to the thrust axis can be calculated for each hemisphere H_k using the relation

$$B_k = \left(\frac{\sum_i |\vec{p}_i \times \vec{n}_T|}{2 \sum_j |\vec{p}_j|} \right) ,$$

where i runs over all of the particles in the hemisphere H_k und j runs over all particles in the event. The two observables are considered, defined by

$$B_t = B_1 + B_2 \quad \text{and} \quad B_w = \max(B_1, B_2)$$

where B_t is the total and B_w is the wide jet broadening.

Sphericity S and Aplanarity A: Both sphericity and aplanarity are based on the eigenvalues of the momentum tensor

$$S_{\alpha\beta} = \frac{\sum_i p_{i,\alpha} p_{i,\beta}}{\sum_i p_i^2} \quad , \quad \alpha, \beta = 1, 2, 3 \quad .$$

where α, β are the spatial co-ordinate labels. The three eigenvalues Q_j of $S_{\alpha\beta}$ are ordered such that $Q_1 < Q_2 < Q_3$. S and A are then defined by

$$S = \frac{3}{2}(Q_1 + Q_2) \quad \text{and} \quad A = \frac{3}{2} Q_1 \quad .$$

C-parameter C: The momentum tensor $S_{\alpha\beta}$ is linearised to become

$$M_{\alpha\beta} = \frac{\sum_i (p_{i,\alpha} p_{i,\beta})/|p_i|}{\sum_i |p_i|} \quad , \quad \alpha, \beta = 1, 2, 3 \quad .$$

The three eigenvalues λ_j of this tensor define C with

$$C = 3(\lambda_1\lambda_2 + \lambda_2\lambda_3 + \lambda_3\lambda_1) \quad .$$

The observed data distributions for the selected events, after correction for backgrounds and for detector effects, are shown in Figs. 3 – 5. The data distributions are compared with those predicted by PYTHIA, HERWIG and ARIADNE version 4.08 [11], at hadron level. The Monte Carlo predictions are in good agreement with the observations.

4.1 Jet rates

Jet rates are defined by means of the Durham clustering algorithm [4] in the following way. For each pair of particles i and j in an event one computes

$$y_{ij} = \frac{2\min(E_i^2, E_j^2)(1 - \cos\theta_{ij})}{E_{vis}^2} \, . \tag{2}$$

The pair of particles with the smallest value of y_{ij} is replaced by a pseudo-particle (cluster). The four-momentum of the cluster is taken to be the sum of the four momenta of particles i and j, $p^\mu = p_i^\mu + p_j^\mu$ ('E' recombination scheme). The clustering procedure is repeated until all y_{ij} values exceed a given threshold y_{cut}. The number of clusters remaining at this point is defined to be the number of jets. Alternatively, one can continue the algorithm until exactly three clusters remain. The smallest value of y_{ij} in this configuration is defined as y_3. In this way one obtains a single

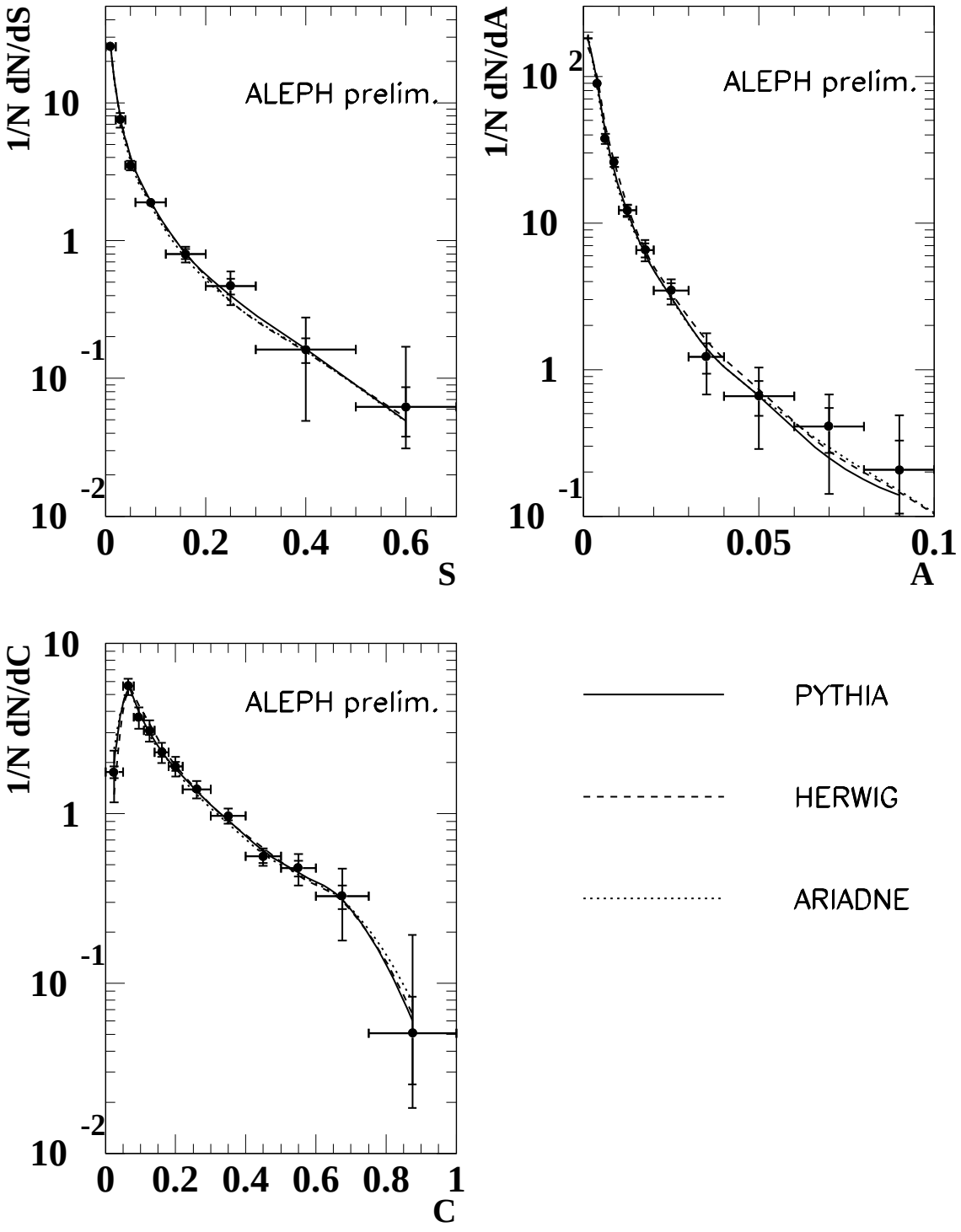

Figure 3: Distributions of Sphericity (S), Aplanarity (A) and C-parameter (C) at 189 GeV. The outer error bars correspond to the quadratic sum of statistical and systematic uncertainties; the inner error bars show the statistical error only.

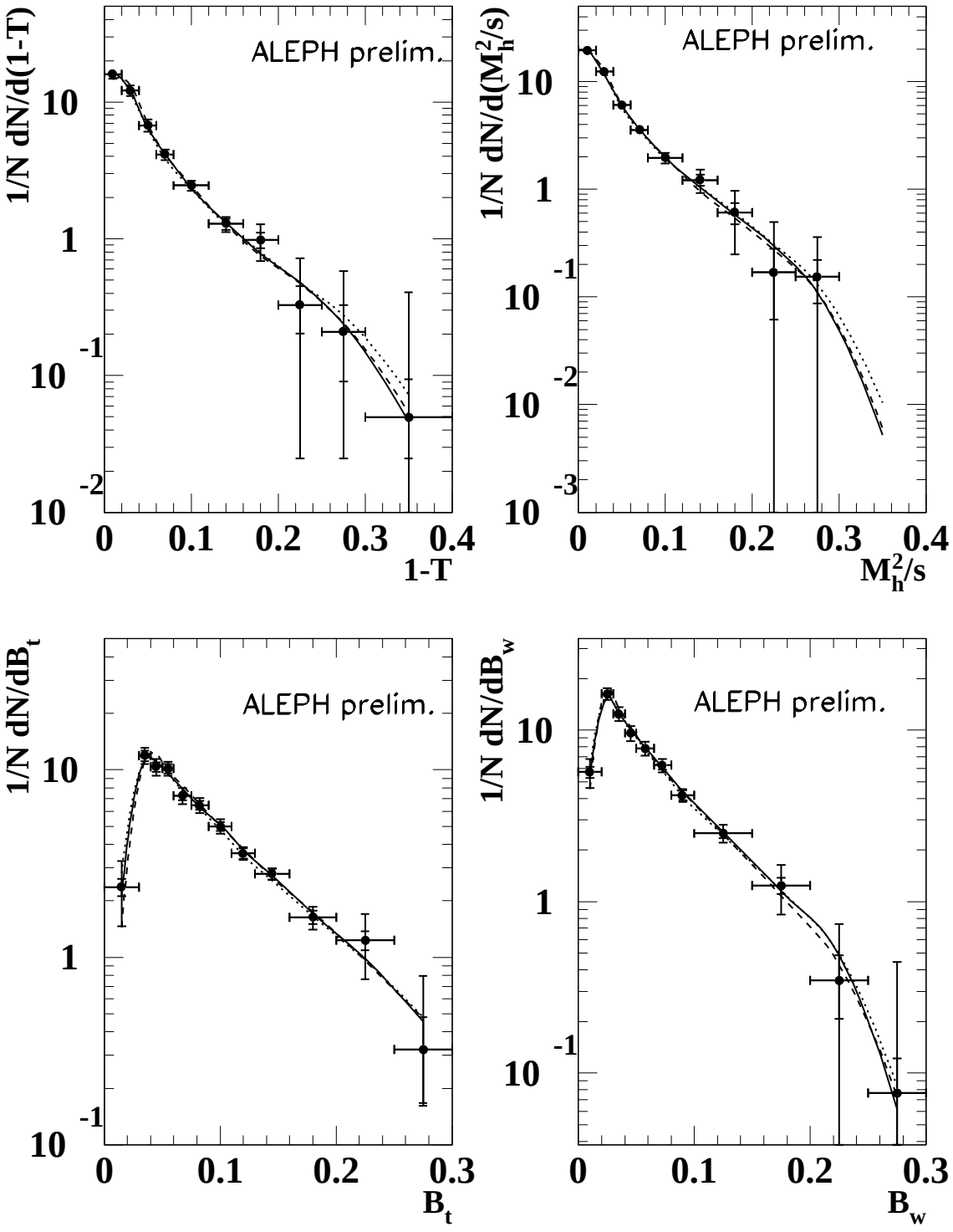

Figure 4: Distributions of 1-Thrust, scaled heavy-jet mass M_h^2/s and the wide-and total-jet broadenings (B_t and B_w) at 189 GeV. The outer error bars correspond to the quadratic sum of statistical and systematic uncertainties; the inner error bars show the statistical error only.

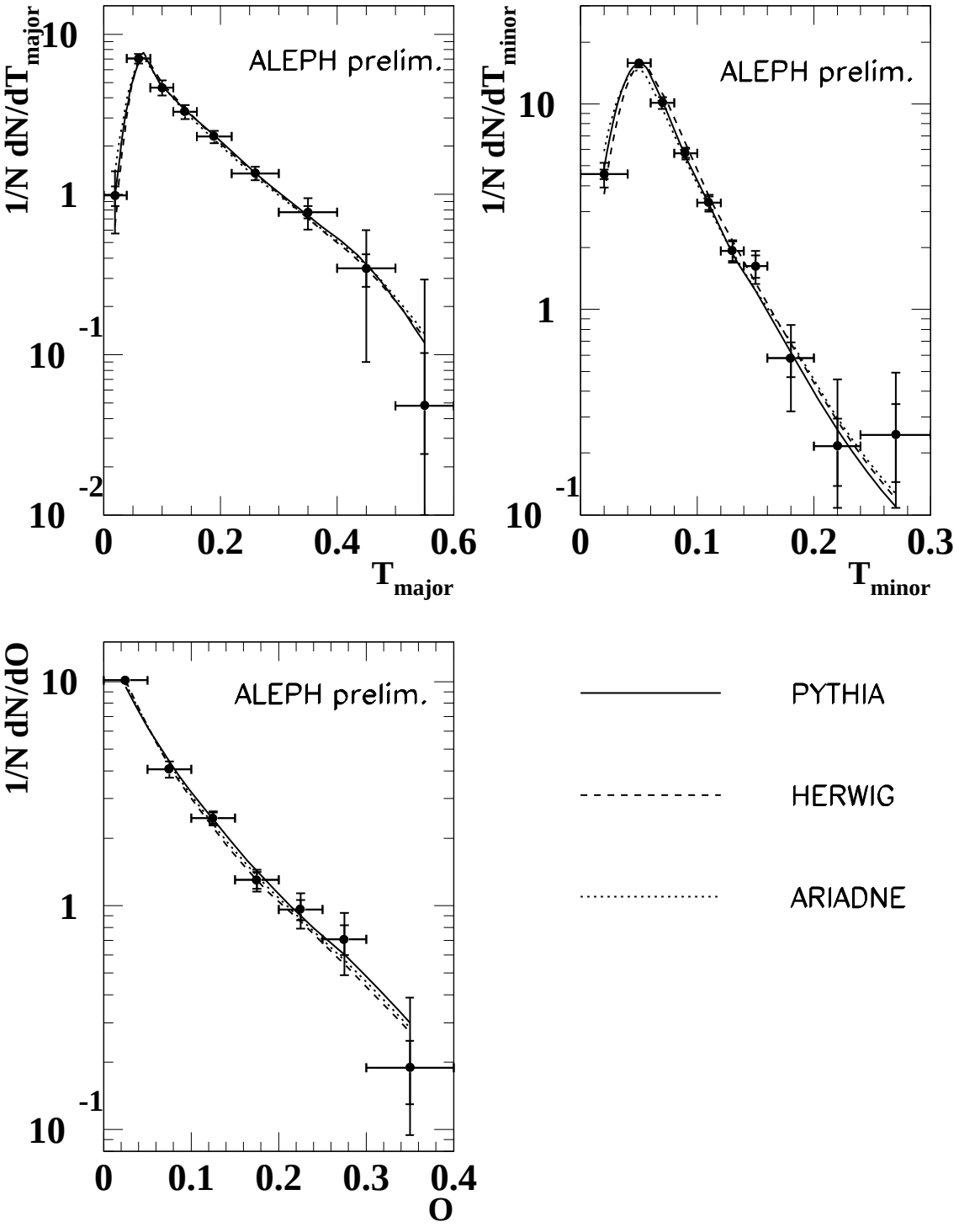

Figure 5: Distributions of $T_{\rm major}$, $T_{\rm minor}$, and Oblateness (O) at 189 GeV. The outer error bars correspond to the quadratic sum of statistical and systematic uncertainties; the inner error bars show the statistical error only.

number for each event, whose distribution is sensitive to the probability of hard gluon radiation leading to a three-jet topology. This can then be used to determine α_s (Section 5).

The n-jet rates were measured for $n = 2, 3, 4, 5$ and $n \geq 6$. Detector correction factors were applied in the same manner as for the event-shape distributions, but here for each value of the jet resolution parameter y_{cut}. Results are shown in Fig. 6 Good agreement with the MC model predictions is observed. Overall, HERWIG is found to provide a somewhat better description of the n-jet rates than PYTHIA.

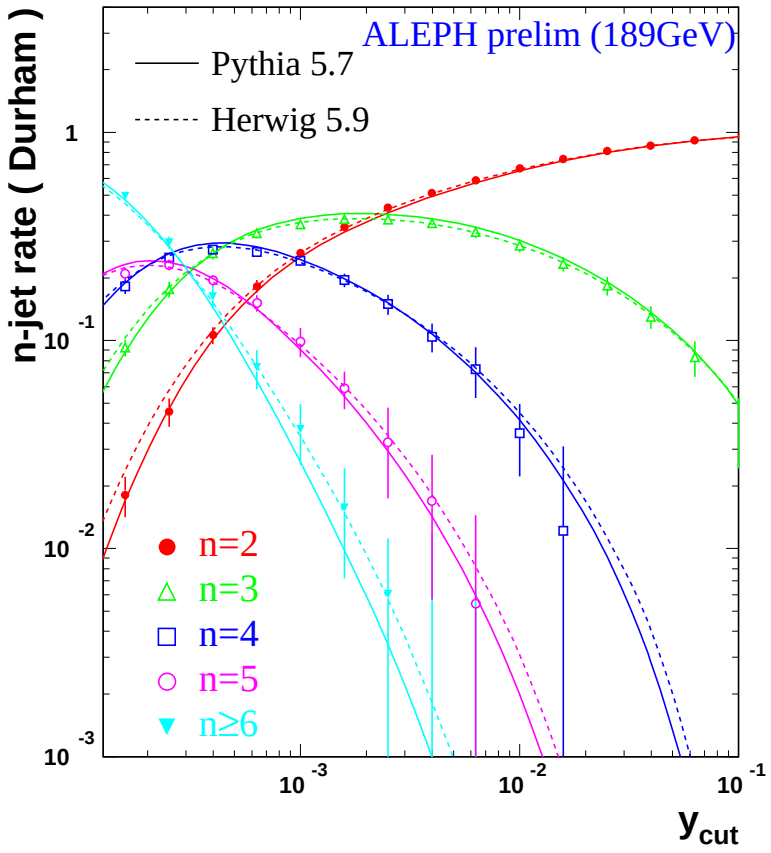

Figure 6: Measured n-jet rates for $n = 2, 3, 4, 5$ and $n \geq 6$ and the predictions of Monte Carlo models, at centre-of-mass energies of 189 GeV.

5 Determination of α_s

QCD predicts that the value of the strong coupling constant, α_s, should decrease by approximately 10% between 91 and 189 GeV. The measurements above the Z resonance are still limited by low event statistics. Therefore the analysis is constructed in such a way that the systematic uncertainties are highly correlated in order to observe best the running of $\alpha_s(Q)$

with the momentum transfer Q, which is equal to the centre-of-mass energy $\sqrt{s}$ in the case of e^+e^-annihilation.

The distributions of the event-shape variables thrust, C-parameter, $-\ln y_3$(Durham scheme) [4], wide jet broadening and heavy jet mass, at 5 different energies including the high-precision measurement at $E_{\rm cm}$= $M_{\rm Z}$ are analyzed in the same way. A binned least-squares fit of the perturbative QCD prediction is repeated for the five event-shape variables at each energy. A larger fit range is chosen than at the previous analyses at $M_{\rm Z}$ [9] in order to minimize the total uncertainty of the high energy measurements.

The distributions of infrared- and collinear-safe observables can be computed in perturbative QCD to second order in α_s using the ERT matrix elements [12] as implemented in the next-to-leading order Monte Carlo generator EVENT2 [13]. In addition, the variables used in this analysis exhibit the property of exponentiation so that leading and next-to-leading logarithms can be resummed to all orders in α_s into analytic functions [14, 15]. These resummed calculations, valid in the semi-inclusive region, have to be matched to the fixed order part in order to obtain an improved prediction over the entire phase space. In the present analysis an improved resummed calculation is used for the wide jet broadening [16], which updates the original work of Ref. [17]. Calculations have also become available for the resummation of the C-parameter [18].

The perturbative fit function is corrected for hadronization effects by means of a transition matrix, which is computed with the PYTHIA Monte Carlo.

The measured distributions are corrected for detector effects, background and remaining ISR contributions as outlined in Section 2.

The value of the renormalization scale is set to $\mu = \sqrt{s}$. Two matching schemes are used, the R-scheme and the Log(R)-scheme [14, 19], and the central value is taken to be the averaged result. Fit results using the R-scheme for four event shape distributions are shown in Fig. 7 and the values of α_s are listed in Table 2 and displayed in Fig. 8. The combined value of α_s at 189 GeV is

$$\alpha_s(189\ \text{GeV}) = 0.1119 \pm 0.0015_{stat} \pm 0.0011_{exp} \pm 0.0030_{theo}.$$

Using the perturbative QCD evolution the corresponding value at $E_{\rm cm}$=$M_{\rm Z}$ is $\alpha_s = 0.1249 \pm 0.0044$.

The experimental systematic errors were estimated as described in Section 2. The theoretical uncertainty on missing higher orders in the perturbative series is estimated in the following way: the renormalization scale is varied in the range $-1 \leq \ln \mu^2/s \leq 1$ for the R matching scheme, which has the larger scale dependence, and the error is taken as the symmetrized difference w.r.t. $\ln \mu^2/s = 0$. Furthermore, half of the difference of the results found for the two matching schemes at $\ln \mu^2/s = 0$ is added quadratically to the error.

The hadronization uncertainty is estimated by using HERWIG and ARIADNE instead of PYTHIA for corrections, and taking the symmetrized difference w.r.t. the results obtained with PYTHIA as an error, which is added in quadrature to the theoretical uncertainties.

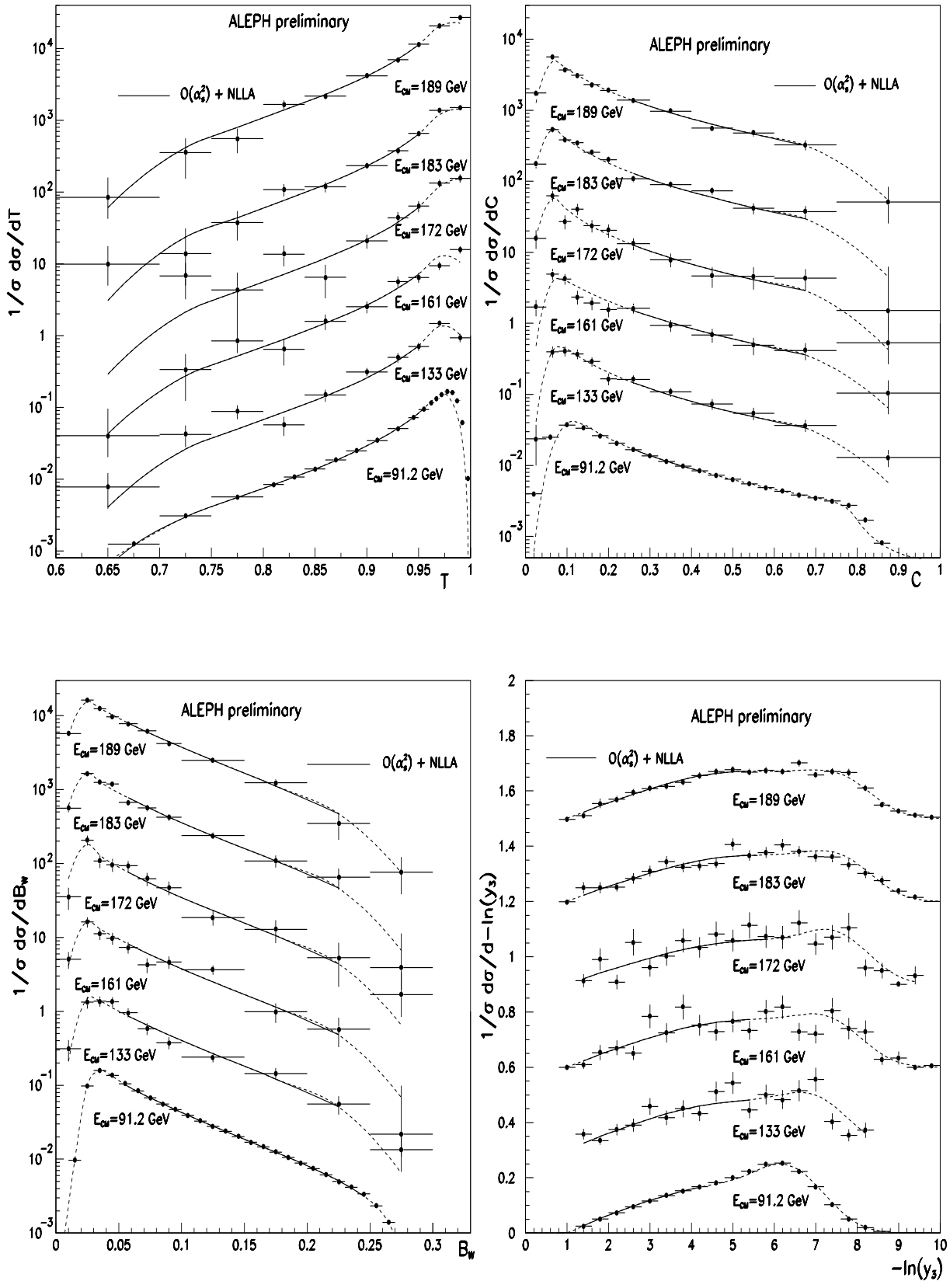

Figure 7: The measured distributions of thrust, C-parameter, wide jet broadening and $-\ln y_3$ at 91.2, 133, 161, 172, 183 and 189 GeV together with the fitted QCD predictions (logR matching scheme). The fit ranges cover the regions indicated by solid lines, the dashed lines show the extrapolation of the QCD prediction. For data points and predictions at different energies scaling factors have been applied in order to show them in one plot.

Table 2: Preliminary results on $\alpha_s(189\ \mathrm{GeV})$ as obtained from fits to distributions of different event-shape variables.

Variable	thrust	wide jet broadening
fit range	0.65 - 0.95	0.06 - 0.24
$\alpha_s(Q)$	0.1167	0.1094
stat. error	0.0025	0.0027
exp. error	0.0008	0.0011
theo. error	0.0028	0.0047
total error	0.0038	0.0056
Variable	C-parameter	heavy jet mass
fit range	0.24 - 0.72	0.08 - 0.25
$\alpha_s(Q)$	0.1133	0.1028
stat. error	0.0027	0.0055
exp. error	0.0011	0.0076
theo. error	0.0034	0.0022
total error	0.0044	0.0097
Variable	$-\log(y_3)$	all combined
fit range	1.2 - 5.2	
$\alpha_s(Q)$	0.1090	0.1119
stat. error	0.0027	0.0015
exp. error	0.0015	0.0011
theo. error	0.0033	0.0030
total error	0.0045	0.0035

6 α_s at different energies

The measurements of α_s have been repeated at lower energies including E_{cm}=M_{Z} using the same variables [20]. These results together with the new result at 189 GeV are shown in Fig. 9. At E_{cm}=M_{Z} second order calculations including quark mass effects are now available [21]. The corresponding corrections to α_s of the order of 1% have been applied. Also shown in Fig. 9 is the three-loop prediction of QCD [22]. The χ^2 for each event-shape fit has been constructed with all error components except the perturbative theoretical error, which is expected to be highly correlated between energy points. The energy dependence is seen to be in good agreement with the predicted running of α_s.

Finally, all measurements at different E_{cm}, as summarized in Table 3, are evaluated at E_{cm}=M_{Z}, using the QCD evolution equation. They are combined using the Best Linear Unbiased Estimator [23] technique. The combined LEP1 and LEP2 result is:

$$\alpha_s(M_{\mathrm{Z}}) = 0.1216 \pm 0.0039$$

7 Conclusions

Preliminary results are presented for analyses of hadronic events recorded by ALEPH at a centre-of-mass energy of 189 GeV. Overall, the measurements show reasonable agreement with the predictions of Monte Carlo models and analytic QCD predictions. The energy evolution of derived

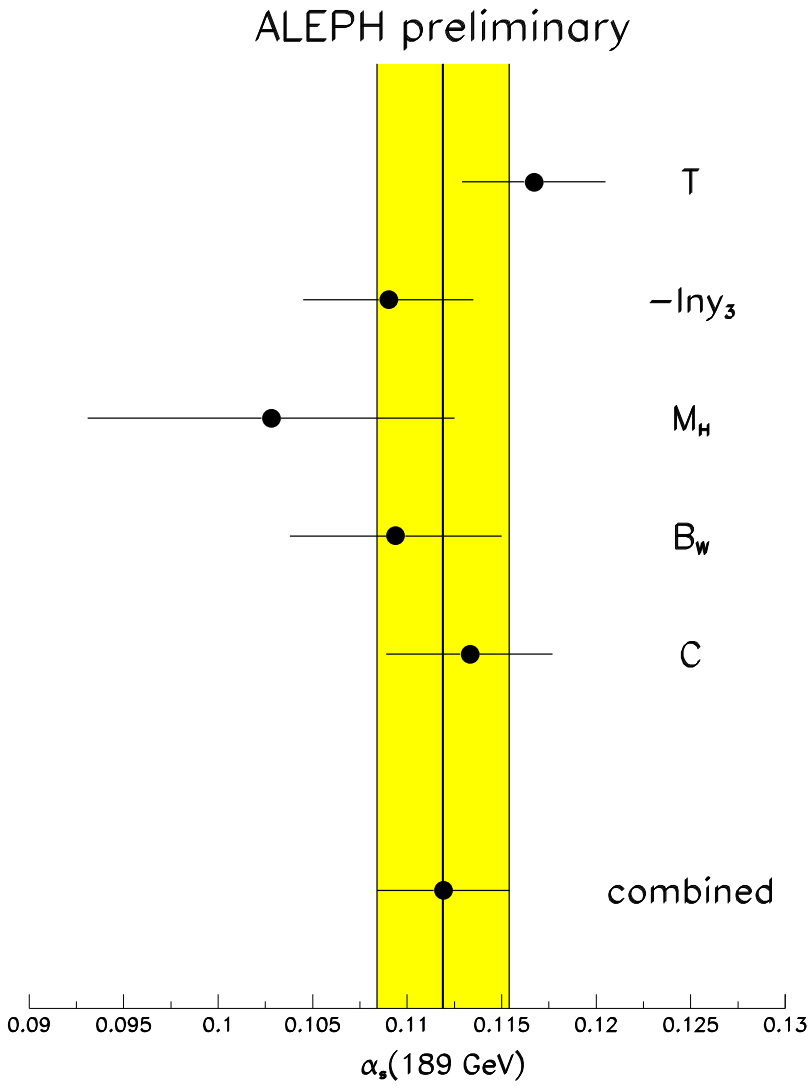

Figure 8: Values of α_s at 189 GeV from different event-shape variables.

quantities such as the mean multiplicity of charged particles $N_{\rm ch}$ and the strong coupling constant α_s has been investigated. For α_s, the energy evolution from $E_{\rm cm} = 91.2$ to 189 GeV is in good agreement with QCD expectations.

Acknowledgements

We wish to thank our colleagues from the accelerator divisions for the successful operation of LEP. It is also a pleasure to thank the technical personnel of the collaborating institutions for their support in constructing and maintaining the ALEPH experiment. Those of the collaboration not from member states thank CERN for its hospitality.

Table 3: Preliminary results on $\alpha_s(Q)$ as obtained from simultaneous fits to all event-shape variables at different energies.

Q [GeV]	91.2	133	161	172	183	189
$\alpha_s(Q)$	0.1229	0.1158	0.1160	0.1064	0.1084	0.1119
stat. error	0.0001	0.0025	0.0045	0.0048	0.0024	0.0015
exp. error	0.0014	0.0008	0.0006	0.0007	0.0009	0.0011
theo. error	0.0044	0.0032	0.0037	0.0024	0.0027	0.0030
total error	0.0046	0.0041	0.0058	0.0054	0.0037	0.0035

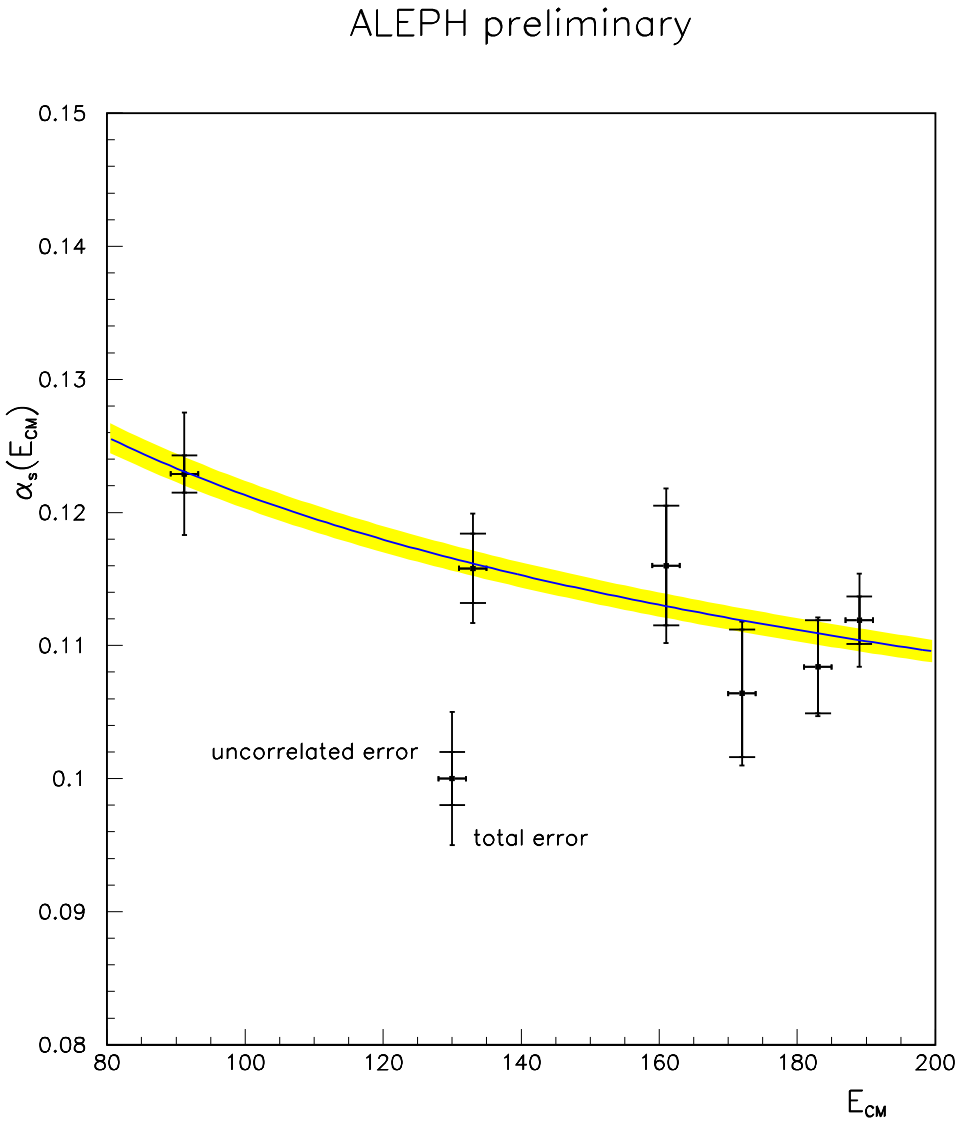

Figure 9: The strong coupling constant α_s measured at 91.2, 133, 161, 172, 183 and 189 GeV using distributions of event-shape variables. The outer error bars indicate the total error. The inner error bars exclude the theoretical error, which is expected to be highly correlated between the measurements.

References

[1] D. Buskulic et al., ALEPH Collab., Z. Phys. C73 (1997) 409.

[2] D. Decamp et al., ALEPH Collab., Nucl. Instr. Meth. A 294 (1990) 121.

[3] D. Decamp et al., ALEPH Collab., Phys. Rep. 216 (1992) 253; D. Buskulic et al., ALEPH Collab., Nucl. Instr. Meth. A360 (1995) 481.

[4] S. Catani et al., Phys. Lett. B269 (1991) 432;
W.J. Stirling et al., Proceedings of the Durham Workshop, J. Phys. G: Nucl. Part. Phys. 17 (1991) 1567;
N. Brown and W.J. Stirling, Phys. Lett. B252 (1990) 657;
S. Bethke et al., Nucl. Phys. B370 (1992) 310.

[5] T. Sjöstrand, Computer Physics Commun. 82 (1994) 74.

[6] S.Jadach, B.F.L. Ward, Z.Was, Comp. Phys. Comm. 79 (1994) 503.

[7] M. Skrzypek, S. Jadach, W. Placzek and Z. Was, Computer Physics Commun. 94 (1996) 216.

[8] G. Marchesini, B.R. Webber, G. Abbiendi, I.G. Knowles, M.H. Seymour, and L. Stanco, Comp. Phys. Comm. 67 (1992) 465.

[9] R. Barate et al., ALEPH Collab., *Studies of Quantum Chromodynamics with the ALEPH Detector*, Physics Reports 294 (1998) 1.

[10] Y.K. Li et al., AMY Collab., Phys. Rev. D41 (1990) 2675;
H.W. Zheng et al., AMY Collab., Phys. Rev. D42 (1990) 737;
W. Braunschweig et al., TASSO Collab., Z. Phys. C45 (1989) 193;
W. Bartel et al., JADE Collab., Z. Phys. C20 (1983) 187;
M. Derrick et al., HRS Collab., Phys. Rev. D34 (1986) 3304.

[11] L. Lönnblad, Computer Physics Commun. 71 (1992) 15.

[12] R.K. Ellis, D.A. Ross and A.E. Terrano, Nuclear Physics B178 (1981) 421.

[13] S. Catani and M. Seymour, Nucl. Phys. B485 (1997) 291.

[14] S. Catani et al., Phys. Lett. B263 (1991) 491;
Phys. Lett. B272 (1991) 368;
Nucl. Phys. B407 (1993) 3.

[15] G. Dissertori and M. Schmelling, Phys. Lett. B361 (1995) 167.

[16] Yu.L. Dokshitzer et al., hep-ph/9801324 (1998).

[17] S. Catani et al., Phys. Lett. B295 (1992) 269.

[18] S. Catani et al., hep-ph/9801350 (1998).

[19] D. Decamp et al., ALEPH Collab., Phys. Lett. B284 (1992) 163.

[20] ALEPH Collab., contribution to ICHEP98, Ref. 940.

[21] P. Nason and C. Oleari, Nucl. Phys. B521 (1998) 237.

[22] R.M. Barnett et al., Particle Data Group, Phys. Rev. D54 (1996) 1.

[23] The LEP Collaborations: ALEPH, DELPHI, L3 and OPAL, Nucl. Inst. Meth. A373 (1996) 101;
L. Lyons, D. Gibaut and P. Clifford, Nucl. Inst. Meth. A270 (1988) 110.